

Electrical characterization of YBCO single crystal surfaces oriented in any crystallographic direction

H. Guillou ^{a,*} J. Chaussy ^a M. Charalambous ^a M. Pissas ^b

^a*CNRS CRTBT, 25 av. des Martyrs, BP166X, 38042 Grenoble Cédex, France.*

^b*Institute of Materials Science, NCRS Demokritos 15310 Ag. Paraskevi, Athens, Greece.*

Abstract

Although considerable studies have been carried out, the true nature of high- T_c superconductors (HTCS) is still not clear. Pseudogap phase at high temperature as well as possible time reversal symmetry breaking at low temperature need further investigations. The need of carefully made samples showing the intrinsic properties of superconductivity is essential to test new theoretical developments. We present in this paper how to control crystallographic orientation in the junction and a technique developed to determine the quality of the interface barrier between a gold electrode and a HTCS : $\text{YBa}_2\text{Cu}_3\text{O}_{7-\delta}$. This potentially allows us to perform Andreev spectroscopy in the CuO_2 planes of cuprate superconductors as a function of temperature, crystallographic orientation and doping.

Key words: cuprates, tunneling, andreev reflexion, ion polishing

PACS: 74.72.Bk, 74.80.Fp, 74.50.+r

1 Introduction

Since their discovery by Bednorz and Müller [1], high- T_c superconductors have been the subject of considerable studies. However, their complex structure and properties are still puzzling solid state physicists [2]. One unanswered question of importance is the relation between the superconducting gap and the pseudogap often seen in ARPES [3,4] and tunneling spectra [5]. Their evolution both in amplitude and symmetry with doping and temperature is of great interest and needs to be determined. Low temperature tunneling studies also showed a possible break of time reversal symmetry [6–8] as well as zero bias anomalies [9–13] whose origin is not clearly established [14,15]. Provided one can distinguish a pseudogap from a superconducting gap, angularly resolved tunneling experiments are good candidates to study these issues. In fact planar junctions are mechanically and chemically stable over the broad range of temperatures necessary to investigate these properties. Moreover, recent arguments [16] suggest that controlling the interface's potential and thus the transport mechanism could allow to determine independantly the energy scales relevant for pairing and phase stiffness [17] in materials where the superconducting density is low such as in HTSC. Thus, the realization of angularly resolved planar contacts with controlled transparency on high- T_c materials could propose experimental answers to still unanswered questions on HTCS. In this article we present a technique that allows us to realize planar junctions with controlled orientation and transparency on YBCO single crystals. We show how to control and characterize the interface quality. Briefly, the junctions are

* Corresponding author : phone : 33 4 76 54 9591

fax : 33 4 76 54 9425

Email address: herve.guillou@ujf-grenoble.fr (H. Guillou).

realized on the side of the crystals and allow direct injection of uncoherent quasi-particles in the copper-oxide planes. The orientation of the junction's plane is set by mechanical polishing of the crystal and the surface barrier is controlled using ion polishing. The junction is geometrically defined using photolithography and conductance spectra $dI/dV(V)$ are measured down to $T = 5\text{K}$ using a lock-in technique. The measurements, carried out on several crystals prepared with different orientations and interface potential, are presented in the third section and interpreted using a phenomenological model. This experiment has an essential advantage : metallic interfaces, obtained after ion polishing, allow us to perform Andreev spectroscopy on YBCO/Au crystallographically oriented planar junctions.

2 Experimental

The $\text{YBa}_2\text{C}_3\text{O}_{7-\delta}$ (YBCO) single crystals used in this work were optimally doped with a T_c of 93 K and a transition width of 0.3 K as measured by ac-Hall susceptibility. The typical crystal size is $500\mu\text{m} \times 300\mu\text{m} \times 80\mu\text{m}$. Crystals with the flattest surfaces and the sharpest corners were selected to be polished. The backleads I_- and V_- are attached to the crystal's rear surface by diffusing silver epoxy at 550°C for one hour in an atmosphere of flowing O_2 as shown in figure 1a). This ensure mechanically robust and electrically excellent contacts.

Since the junctions will be realized so as to inject current directly in the CuO_2 planes the junction plan must include the \vec{c} axis. In orther words, we must be able to cut the crystal in a controllable manner in order to expose a surface less than $100\mu\text{m}$ thick on its side. Polishing seems the simplest solution. The sample is embedded in an epoxy matrix in order to minimize side effects

during polishing. Prior to casting, the crystal is oriented and attached to a copper disk to ensure a good thermal contact. The orientation is controlled within a couple of degrees with respect to the CuO_2 planes and within $\pm 7^\circ$ with respect to the c-axis. This uncertainty is much lower than the current injection cone, usually estimated to be around $\pm 15^\circ$ [18] for low transmission interfaces. After polymerization, the whole epoxy block is carefully polished with fine diamond paste. Great care has been taken in order to avoid chemical attack of crystals (water-free polishing), cracks (low speed spinning), diamond inclusions and rounded surfaces (low pressure). Between each stage the sample is washed in an ultrasonic bath and rinsed with pure acetone and ethanol to avoid contamination. The resulting surface is flat and without any scratches as observed with a DIC microscope. Some surfaces were observed using AFM and the measured surface roughness was found to be around 15 Å and sample independant. A typical image is shown on the figure 1b). The scanning size did not significantly change the measured roughness. It has been pointed out by Walker *et al.* [14] that diffuse scattering at the interface can significantly complicate the transmission process. Thus it is crucial to keep the roughness comparable with the Fermi wavelength of the charge carriers in YBCO. We note that very little care has yet been taken to communicate the structural properties of the surface on which planar junctions are elaborated, even though a parameter such as roughness is crucial to predict the transport properties of junctions. The measured roughness is only twice the carrier wavelength and although some charge carriers probably undergo diffuse scattering, polishing of YBCO surface yields outstanding results concerning the surface's morphology.

At this stage the flat and smooth crystal surface is ready to be used to elaborate the junctions. However, polishing induces a fine amorphous or deoxy-

generated layer directly below the surface. Since we are concerned with conserving the bulk properties of superconductivity throughout the sample, this layer must be removed. Ion beams have been used by several groups to smooth YBCO films [19], to improve superconducting properties of epitaxial YBCO films [20] and to pattern, without damage, YBCO thin films [21]. In line with these results we used low energy (300 eV) Xe ion beams at a normal incidence to polish and improve the superconducting properties of the crystal surface. The polishing efficiency is related to the sputtering yield of the impinging ions. This has recently been reviewed [22] and it appears that for normally incident ions, the sputtering yields are maximum for a surface oriented roughly 60° off the normal. Therefore this treatment erodes these asperities and improves the surface roughness, as well as removes the degraded surface layer. It is well known that the superconducting properties of cuprates are very sensitive to oxygen contents. During the ion beam polishing a large amount of energy is dissipated in the surface's vicinity. To avoid heating and further loss of oxygen during the ion beam polishing the crystal is maintained at liquid nitrogen temperature. After ion polishing, a 150 nm thick gold layer is sputtered *in-situ* and will be used as a counter electrode.

We are interested in the transport properties of the YBCO/Au interface. The geometry of the junction and the leads that are attached to it are defined using a photolithographic process and are shown in figure 2. The nominal junction surface is $S = 0.18 \cdot 10^{-3} \text{ cm}^2$. The gold resistivity is of the order of $0.1 \mu\Omega \cdot \text{cm}$ at low temperature. For a uniform current injection, this requires an interface resistance higher than $4 \cdot 10^{-6} \Omega \cdot \text{cm}^2$ for the nominal junction dimensions [23–25]. This condition was always fulfilled and the only source of inhomogeneities in the current injection is the inhomogeneity of the superconductor's surface.

The measurement temperature can be varied from 5 K to 150 K, the current is measured as a function of the bias voltage and the slope of the $I(V)$ characteristic is measured using a lock-in technique. The experimental setup gives an absolute value of the dynamic conductance as shown in the inset in figure 5a).

In this article we stress the fact that the transparency of the YBCO/Au interface can be controlled by choosing the method of preparation of the junctions. In fact we compare in the next section the results obtained on crystals prepared differently. Two behaviours were observed depending on the preparation technique : i) the gold counter-electrode is directly sputtered after the *mechanical* polishing. This leads to an insulating behaviour of the interface resistance and thus a tunnel effect at low temperature. ii) The counter-electrode is evaporated *in-situ* after low temperature and low energy *ion* polishing. This leads to a metallic behaviour of the interface resistance and hence Andreev effect at low temperature.

3 Results and discussion

When considering an interface between two materials, the transmission coefficient can be estimated in principle from the absolute value of the surface resistivity. For high temperature superconductors in contact with a normal metal this is estimated [26,27] to be $R_{c\square} = (\hbar/e^2) \times 2\pi^2/Dk_F^2$ where $R_{c\square}$ is the measured surface resistivity, k_F the Fermi wave vector of carriers in the superconductor and D the transmission coefficient. For an ideal interface where $D = 1$ and a Fermi wave vector $k_F \sim 10^{-8} \text{ cm}^{-1}$ the estimation gives $R_{c\square} \sim 10^{-11} \Omega \cdot \text{cm}^2$. Numerous experiments have been designed to reach this ideal limit but the best results [28,29] gave interface resistances 100 times

larger than the theoretical estimate. To explain this discrepancy Mannhart *et al.* [30] proposed the existence of a depletion layer near the interface that tends to enhance the interface resistance. Moreover spatially resolved measurements of the proximity effect [31] induced in thin gold layers showed large inhomogeneities. More recent STS measurements [32] on high quality $\text{Bi}_2\text{Sr}_2\text{CaCu}_2\text{O}_{8-\delta}$ thin films showed quasi-particles spectra going from S-I-N tunneling to Semi-C-I-N on a scale of a few nm. These results show that calculating the transmission coefficient from resistance measurements of macroscopic interfaces is difficult mainly because of intrinsic large inhomogeneities on high temperature superconductor surfaces.

In order to determine the dominant transport mechanism through the interface, the sole knowledge of the interface resistance is insufficient. However its temperature dependance provides indications on which transport mechanism dominates. Indeed, it is reasonable to describe the junctions as an insulating and a metallic layer. If the two layers are in serial an insulating behaviour is expected for low enough temperatures. On the contrary if the two layers are in parallel a metallic behaviour is expected for low enough temperatures as shown in fig. 3). From these properties we deduce the dominant transport mechanism through the interface. At low temperatures, a metallic interface will show Andreev reflections whereas an insulating interface will show tunneling effects. Fig. 4) shows the temperature dependance of the interface resistance for different bias voltages for the two preparation procedures for a (110) oriented surfaces.

For fig 4a) the surface of the crystal was simply mechanically polished and carefully cleaned. The junction resistance increase for decreasing temperatures is characteristic of insulating properties. Tunneling will be the dominant trans-

port mechanism through the interface at low temperatures. We note that the behaviour of the resistance at zero bias is different from the ones at finite bias. The increase of conductivity for low bias is the signature of a Zero Bias Conductance Peak (ZBCP). ZBCP's in HTSC are explained either in the Andreev Bound States [9] mechanism, or in the presence of surface defects that create Impurity Bound States [15]. Although these different origins can in principle be differentiated by their different magnetic field properties, their probable coexistence does not facilitate the determination of their contribution to the global ZBCP. The curves in fig. 4b) show a clear metallic behaviour of the junction's resistance with temperature. The junction was made *in situ* after ion polishing. The metallic behaviour comes from the removal of the degraded layer at the surface by the ions. Thus at low temperature we expect to measure mostly Andreev transport through the interface.

The fig. 5) shows the measured spectra for the tunneling and the Andreev limit obtained on different crystals. For the two junctions shown here the current injection was along the line of node of a $d_{x^2-y^2}$ order parameter. In the tunneling limit (fig. 5a), the spectra show all the expected qualitative features of a d -wave superconductor : *i*) the DOS is depreciated below an energy of about 25 meV corresponding to the gap amplitude generally found in the literature and *ii*) the ZBCP is present and similar to the common ZBCP measured on HTCS[10]. In the metallic limit, the conductance is enhanced at low bias and has a sharp point at zero bias indicative of a d -wave superconductor.

4 Conclusion

We realized and characterized planar junctions on the side of YBCO single crystals. The direction of the injected current is controlled within a few degrees in CuO₂ planes. We showed that the interface barrier can be changed from insulating to metallic by using different preparation techniques. If the crystal is simply polished the resulting interface will be insulating and single electron tunneling will be the main mechanism of transport through the interface. On the other hand, if the surface undergoes an ion polishing stage it will show a metallic behaviour and Andreev reflections below the superconducting transition. The mechanical stability of the junction allows us to perform Andreev spectroscopy as a function of temperature. These investigations are currently being undertaken and will be published elsewhere. They could provide some experimental evidence of the ideas suggested by Deutscher [16] by measuring different energy scales for pairing (tunneling spectroscopy) and phase coherence (Andreev spectroscopy). Our results show that under carefully established conditions the control of the surface potential of HTCS can be achieved. Further research to understand HTCS require the use of controlled interfaces. The technique presented here has yielded goog results. The authors would like to thank T. Fournier and P. Brosse-Marron for technical support and O. Fruchart for initial help with the AFM work, H. G. thanks B. Lussier for early supervision.

References

- [1] Bednorz J.G., Müller K.A., Z. Phys. B 64 (1986) 189.

- [2] Orenstein J., Millis A.J., Advances in the Physics of High-Temperature Superconductivity, *Science* 288 (2000) 468.
- [3] Loeser A.G., Shen Z.-X., Dessau D.S., Marshall D.S., Park C.H., Fournier P., Kapitulnik A., Excitation Gap in the Normal State of Underdoped BSCCO, *Science* 273 (1996) 325.
- [4] Pavuna D., Vobornik I., Margaritondo G., Photoemission Experiments on High- T_c Superconductors: Recent Progress and Some Open Questions, *J. Supercond.* 13 (5) (2000) 749.
- [5] Renner Ch., Revaz B., Kadowaki K., Maggio-Aprile I., Fischer O., Observation of the Low Temperature Pseudogap in the Vortex Core of Bi2212, *Phys. Rev. Lett.* 80 (16) (1998) 3606–3609.
- [6] Sharoni A., Koren G., Millo O., Correlation of tunneling spectra with surface nano-morphology and doping in thin YBCO films, prépublication *Europhysics Lett.* cond-mat/0103581.
- [7] Covington M., Aprili M., Paraoanu A., Greene L. H., Observation of Surface-Induced Broken Time-Reversal Symmetry in YBCO Tunnel Junctions, *Phys. Rev. Lett.* 79 (2) (1997) 277–280.
- [8] Folgelström M., Rainer D., Sauls J. A., Tunneling into Current-Carrying Surface States of High- T_c Superconductors, *Phys. Rev. Lett.* 79 (2) (1997) 281–284.
- [9] Hu Chia-Ren, *Phys. Rev. Lett.* 72 (10) (1994) 1526–1529.
- [10] Alff L., Kleefisch S., Schoop U., Andreev bound state in high temperature superconductors, *Eur. Phys. J. B* 5 (1998) 423–438.
- [11] Lesueur J., Greene L.H., Feldmann W.L., Inam A., Zero bias anomalies in YBCO tunnel junctions, *Physica C* 191 (1992) 325–332.

[12] Aprili M., Badica E., Greene L. H., Doppler Shift of the Andreev Bound States at the YBCO Surface, *Phys. Rev. Lett.* 83 (22) (1999) 4630–4633.

[13] Krupke R., Deutscher G., Anisotropic Magnetic Field Dependence of the Zero-Bias Anomaly on In-Plane Oriented [100] YBCO/In Tunnel Junctions, *Phys. Rev. Lett.* 83 (22) (1999) 4634.

[14] Walker M.B., Pairor P., Universal Width for the ZBA, *Phys. Rev. B* 60 (14) (1999) 10395–10399.

[15] Samokhin K.V., Walker M.B., Localized surface states in HTSC : alternative mechanism of zero-bias conductance peaks, *Phys. Rev. B* 64 (17) (2001) 172506.

[16] Deutscher G., Coherence and single-particle excitations in the high-temperature superconductors, *Nature* 397 (1999) 410–412.

[17] Emery V. J., Kivelson S. A., Importance of phase fluctuations in superconductors with small superfluid density, *nature* 374 (1995) 434.

[18] Wolf E.L., *Principles of Electron Tunneling Spectroscopy*, Oxford University Press, 1985.

[19] Hebard A.F., Fleming R.M., Short K.T., White A.E., Rice C.E., Levi A.F.J., Eick R.H., Ion beam thinning and polishing of YBCO films, *App. Phys. Lett.* 55 (18) (1989) 1915–1917.

[20] Chen L., Yang T., Nie J.C., Wu P.J., Huang M.Q., Liu G.R., Zhao Z.X., Enhancement of superconductivity by low energy Ar ion milling in epitaxial YBCO thin films, *Physica C* 282–287 (1997) 657–658.

[21] Xavier P., Fournier T., Chaussy J., Richard J., Charalambous M., Nonperturbative ion etching of YBCO thin films, *J. Appl. Phys.* 75 (2) (1994) 1219–1221.

[22] Carter G., The Physics and applications of ion beam erosion, *J. Phys. D: Appl. Phys.* 34 (2001) 1.

[23] Rzchowski M.S., Wu X.W., Bias dependence of magnetic tunnel junctions, *Phys. Rev. B* 61 (9) (2000) 5884–5887.

[24] van de Veerdonk R.J.M, Nowak J., Meservey R., Current distribution effects in magnetoresistive tunnel junctions, *Appl. Phys. Lett.* 71 (10) (1997) 2839–2841.

[25] Pedersen R.J., Vernon Jr. F.L., Effect of film resistance on low-impedance tunneling measurements, *Appl. Phys. Lett.* 10 (1) (1967) 29–31.

[26] Deutscher G., Proximity effects with the cuprates, *Physica C* 185–189 (1991) 216–220.

[27] Kupriyanov M.Yu., Likharev K.K., Towards the quantitative theory of the High- T_c Josephson junctions, *IEEE Trans. Magnetics* 27 (2) (91) 2460–2463.

[28] Tsai J.S., Takeuchi I., Tsuge H., anomalous interface resistance between oxyde superconductors and noble metals, *Physica B* 165–166 (1990) 1627–1628.

[29] Jing T.W., Wang Z.Z., Ong N.P., Gold contacts on superconducting crystals of YBCO with very low contact resistivity, *Appl. Phys. Lett.* 55 (18) (1989) 1912–1914.

[30] Mannhart J., Hilgenkamp H., interfaces involving complex superconductors, *Physica C* 317–318 (1999) 383–391.

[31] Koyanagi M., Kashiwaya S., Akoh H., Kohjiro S., Matsuda M., Hirayama F., Kajimura K., Study of YBCO/Au surface using LTSTM/STS, *Jpn. J. Appl. Phys.* 31 (11) (1992) 3525–3528.

[32] Cren T., Roditchev D., Sacks W., Klein J., Moussy J.-B., Deville-Cavellin C., Laguës M., Influence of Disorder on the Local Density of States in High- T_c Superconducting Thin Films, *Phys. Rev. Lett.* 84 (1) (2000) 147–150.

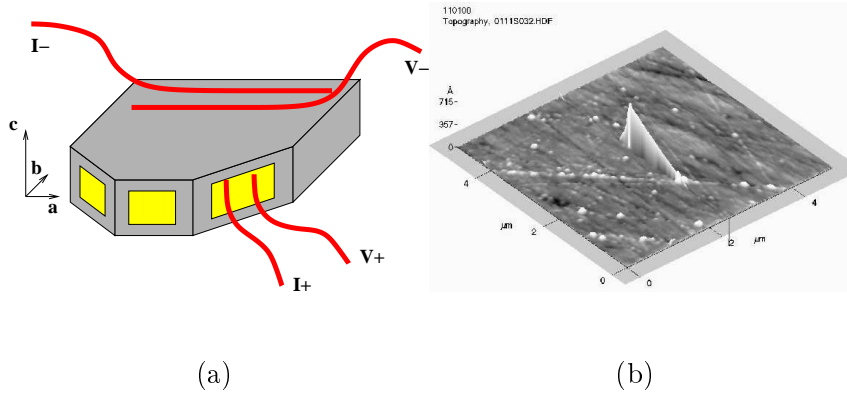


Figure 1. The junctions are realized on a plane containing the c -axis of the crystal (left). The orientation of the surface is controlled and determined by mechanical polishing that yields very small roughness as shown with AFM (right). (a) Planar junctions on the "side" of YBCO single cristal. (b) AFM scan of the mechanically polished surface. The RMS roughness is about 1–2 nm.

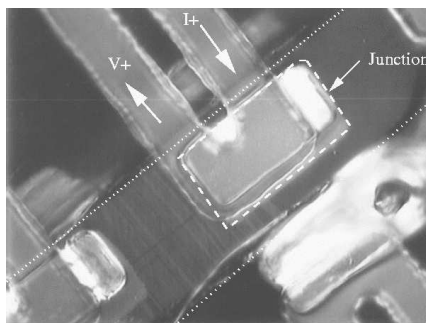


Figure 2. Contact and probes geometry. The crystal boundaries are underline by the dotted lines. The junction is realized within the discontinuous line. The contact nominal surface is $S = 30\mu\text{m} \times 60\mu\text{m}$.

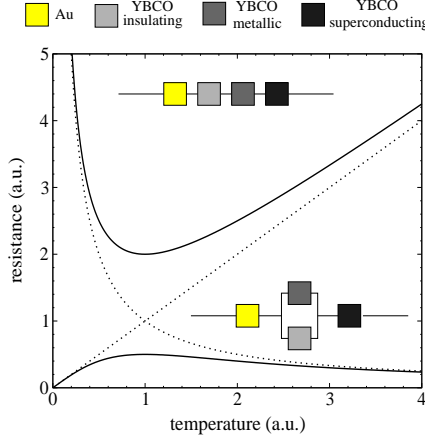


Figure 3. Modeling of the interface between YBCO and a normal metal. Top: all the layers are in series. The resistance vs T has positive curvature: $R(t) = \alpha(1/t) + \beta t$. Bottom: the insulating and metallic layers are in parallel. The resistance vs T has a negative curvature: $R(t) = 1/(\alpha(1/t) + \beta t)$.

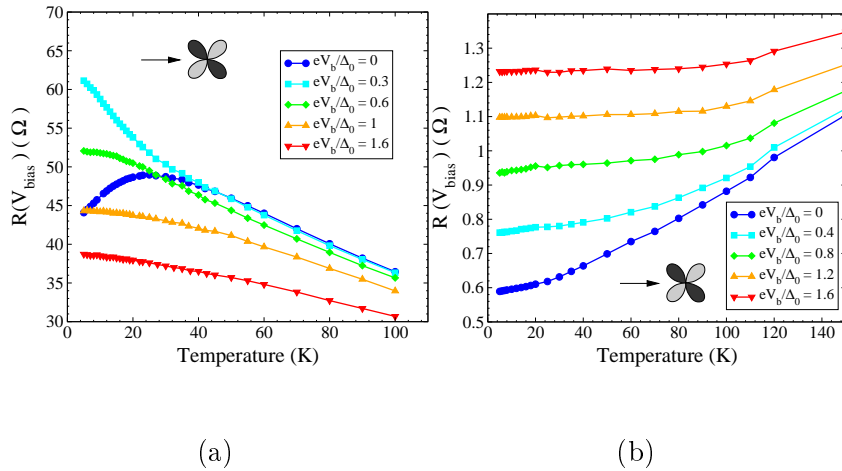


Figure 4. Evolution with temperature of the resistance for a bias voltage V_b . The junctions are realized on a (110) oriented surface. The two different behaviours observed are related to the preparation techniques. (a) Insulating (tunnel) limit obtained when the crystal is only mechanically polished. (b) Metallic regime obtained after ion polishing of the crystal's surface.

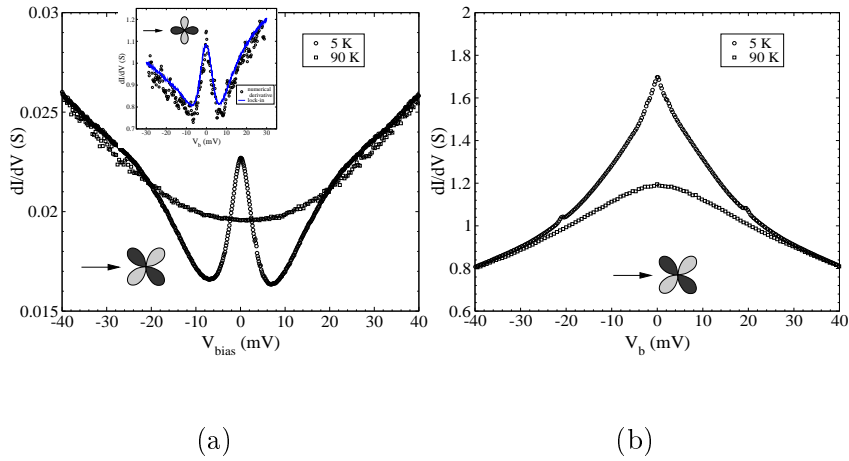


Figure 5. Dynamic conductance spectra obtained for $\text{YBa}_2\text{Cu}_3\text{O}_{7-\delta}(110)/\text{Au}$ junctions for different transport regime through the interface. The spectra measured at 90 K were shifted by a constant to overlay the spectra measured at 5 K. The absolute values can be determined from the fig. 4). (a) tunneling spectrum obtained at low temperature; inset : comparaison of the measured dynamic conductance and the one computed from the numerical derivative of the $I(V)$ curve (not shown). (b) Andreev spectra obtained after ionic polishing of the cristal surface